Journal of Hydrology 582 (2020) 124489

Contents lists available at ScienceDirect

Journal of Hydrology

journal homepage: www.elsevier.com/locate/jhydrol

Research papers

Comparison of soil hydraulic properties estimated from steady-state experiments and transient field observations through simulating soil moisture in regenerated *Sphagnum* moss

James Elliott*, Jonathan Price

Department of Geography and Environmental Management, University of Waterloo, Waterloo, ON N2L 3G1, Canada

A R T I C L E I N F O

This manuscript was handled by P. Kitanidis, Editor-in-Chief, with the assistance of Jiri Simunek, Associate Editor

Keywords:
HYDRUS
RETC
Sphagnum
Unsaturated properties
Curve fitting
Inverse modelling

A B S T R A C T

Growing *Sphagnum* moss for peatland restoration and fibre farming requires the proper moisture regime be maintained; thus, there is a desire to optimize growth by creating ideal hydrological conditions. However, it is uncertain which parameterization method is most suitable to describe field-scale processes and which soil water retention model and hydraulic conductivity curve (approach) is the most acceptable to use. Parameterizations of the van Genuchten – Mualem (VGM) equation were done using RETC, curve fitting to direct measurements of the water retention and unsaturated hydraulic conductivity curves; and Hydrus-1D, inverse modelling to field observations of soil moisture. The acceptability of each parameterization was tested by comparing soil moisture estimates based on forward simulations to observed soil moisture in two regenerated moss profiles, established in 1970 and 2006 cases, respectively. The transient field model simulated soil moisture well, and had an RMSE of 0.05 and 0.06 for 1970 and 2006, respectively. The most error occurred during the wettest and driest periods of the simulations. Simulated soil moisture was consistently drier than the observed soil moisture, in the steady-state laboratory simulation, and had markedly higher RMSE, 0.14 and 0.27 for the 1970 and 2006 profiles, respectively. The estimate of the VGM α parameter, an approximately the inverse of the air-entry pressure, fit to direct measurements of the retention and unsaturated hydraulic conductivity curves was an order of magnitude higher than that fit to field observation. The results of the simulation suggest that inverse modelling to field soil moisture should be used to estimate VGM parameters to more accurately represent field-scale soil moisture dynamics.

1. Introduction

Unsaturated zone hydrological process in peat and *Sphagnum* mosses have become a topic of increased interest over the past two decades because of their importance to horticultural applications (da Silva et al., 1993), climate change resilience (Moore and Waddington, 2015), restoration (McCarter and Price, 2015), and carbon dynamics/plant growth (Strack and Price, 2010). Unsaturated zone properties control the ability of a porous media to retain and conduct water under negative pressure head, which is dictated by morphology of the pore network and water distribution within it (Jerauld and Salter, 1990), the wettability and saturation history of the media (Man and Jing, 1999), and the pore size distribution of the media (Mualem, 1976; van Genuchten, 1980). *Sphagnum* mosses are the dominant species in many peatlands, and the pore network is the space between overlapping leaves and branches (Hayward and Clymo, 1982). *Sphagnum* mosses are bryophytes that have no roots, which rely on water conveyed through the pore network under capillary force. Thus, understanding unsaturated process and properties is important to understand how peatlands develop, function, and persist.

Recently, *Sphagnum* fibre farming is being considered as an alternate management plan to restoring peatlands after they have been disturbed for peat harvesting (Brown et al., 2017) or agriculture (Gaudig et al., 2018). The objective of fibre farming is to maximize *Sphagnum* biomass accumulation by optimizing water availability, which can be done with a variety of irrigation systems (e.g. Brown et al., 2017; Gaudig et al., 2018). The optimum water content for *Sphagnum* moss is available to maximize carbon uptake through photosynthesis (Flanagan, 1996; Silvola, 1990), but not restrict gas exchange (Silvola, 1990). Furthermore, water table stability of the peatland is an important factor in moss photosynthesis and biomass production (Brown et al., 2017; Pouliot et al., 2015). Hydrological models are a useful tool for assessing

* Corresponding author.
E-mail address: jbelliot@uwaterloo.ca (J. Elliott).

https://doi.org/10.1016/j.jhydrol.2019.124489
Received 23 July 2019; Received in revised form 12 December 2019; Accepted 16 December 2019
Available online 19 December 2019

the scalability of an operation, and how moss growth and species composition may change the water demand and irrigation strategies.

Simulations, which use unsaturated hydrological models, can be used to assess water availability; the models are defined by the relationships between pressure head (ψ), soil moisture (θ), and hydraulic conductivity (K). For organic soils, retention curves ($\theta(\psi)$) and hydraulic conductivity curves ($K(\psi)$) have typically been derived by parameterizing soil hydraulic property functions to laboratory observations (da Silva et al., 1993; Gnatowski et al., 2002; Price et al., 2008). Parameters describing soil hydraulic properties have usually been used to compare the retention capacity of different soils (Gnatowski et al., 2010; Moore et al., 2015) or assess the functional differences of mosses (Gauthier et al., 2018; Golubev and Whittington, 2018; McCarter and Price, 2014). Furthermore, hydrological models have also been used to characterize unsaturated zone contaminant transport (Gharedaghloo et al., 2018; Simhayov et al., 2018), plant stress (Moore and Waddington, 2015), and evaporation from peatlands (Dixon et al., 2017). Very little work has been done to predict soil hydraulic parameters which describe field-scale soil moisture (Schwärzel et al., 2006a, 2006b).

The use of soil water characteristic and hydraulic conductivity curves in models requires that a function is fit to the $\theta(\psi)$ and $K(\psi)$ observations. Traditionally, multi-step outflow experiments using pressure cells (e.g. Weiss et al., 1998) were only able to generate the data to fit the retention curve. More recently, the tension disk method was developed, which allows for the direct observation of the retention and hydraulic conductivity curves (Price et al., 2008). Numerous studies have measured the retention and hydraulic conductivity curves but have not used the data for curve fitting (e.g. Goetz and Price, 2015; McCarter and Price, 2015). An alternative approach to directly fitting the soil water retention and hydraulic conductivity curves is inverse modelling, which is the process of iteratively solving Richards equation to best match transient observations of soil moisture and/or pressure head (Vrugt et al., 2008; Weber et al., 2017a). Inverse modelling for organic soils has been done in the laboratory using multi-step outflow (Gnatowski et al., 2010), evaporation (Weber et al., 2017a), and unsteady state displacement experiments (Gharedaghloo and Price, 2019). Additionally, inverse modelling can be done using observations from field experiments (Schwärzel et al., 2006a, 2006b). Parameters determined using direct curve fitting differed from those determined with inverse modelling, the modelled curve suggests that drainage occurs closer to 0 cm of pressure (Schwärzel et al., 2006a); these differences will be discussed later. Studies with mineral soils have found that parameterization with inverse modelling produced more accurate retention curves than parameters fit with direct curve fitting (Lier, 2019; Morvannou et al., 2013).

Despite the large volume of work done to characterize unsaturated properties in the laboratory, virtually no attempts have been made to assess their validity in field conditions (e.g. Schwärzel et al., 2006b). Furthermore, several laboratory measurement methods have been presented and the evidence suggests that they can result in different parameter estimates (Schelle et al., 2013), and that there can be large discrepancies in their performance in a field setting (Schwärzel et al., 2006b). An improved understanding of unsaturated properties can be gained by assessing how different parameter fitting methods can simulate water retention and transport in a soil column. The intent of this study is to determine the VGM parameters that accurately describe soil moisture dynamics in the field. Therefore, the objectives are (a) to determine VGM parameters for regenerated *Sphagnum* moss profiles using direct curve fitting and inverse modelling; and (b) assess how effective each parameter set is at simulating soil moisture during the summer field season using a one dimensional hydraulic model.

2. Methods

2.1. Study site and sample preparation

Data for this study were originally collected and published by Taylor and Price (2015); for a full description of methods consult the original publication. The study site was a cutover peatland located south of Shippagan, New Brunswick (47°40′N, 64°43′W) and it is characterized by alternating raised baulks and lowered trenches as a result of traditional block-cut peat harvesting. Since abandonment in 1970, *Sphagnum* mosses spontaneously recolonized the trenches. Additionally, the site was selected for research in *Sphagnum* fibre farming. Beginning in 2004, plots of vegetation were removed and replanted with *Sphagnum* mosses every two years until 2010 (Landry and Rochefort, 2009). Plot names indicate the year of abandonment (1970) or the year where *Sphagnum* was planted. The profile at each plot was old cut-over peat overlain by moss layers of varying thickness reflecting the time since moss re-establishment (Taylor and Price, 2015). To measure soil moisture, triplicate CS605 TDR probes were installed at depths of 2.5, 7.5, 12.5, and 17.5 cm; and 2.5, 7.5, and 12.5 cm for the 2006 and 1970-C plots, respectively. Soil moisture was measured hourly, with the exception of TDRs installed at 12.5 and 17.5 cm below the surface in the 2006 profile, which were manually measured several times a week (Taylor and Price, 2015). Calibration of the TDRs was done gravimetrically, for more information see Taylor and Price (2015) for a full description of the calibration process. Meteorological, soil moisture, and water table data were collected hourly at the 1970-C and 2006 plots. Although the 2010 plot was instrumented, the moss layer was not thick enough to be instrumented or adequately sampled, thus, it was not used in this study. Several experimental plots were established in regions with moss growth starting in 1970 (Taylor and Price, 2015); since only the 1970-C plot was instrumented, it will be referred to as 1970 in this study. Samples of *Sphagnum* moss (n = 2 per profile) and cut-over peat (n = 1 per profile) were taken from the top 10 cm, the base of the moss profile and the cut-over peat of each plot; depths represent the midpoint of samples that had a height of 5 cm (Fig. 1). Soil water retention and unsaturated hydraulic conductivity were determined in the laboratory (Taylor and Price, 2015) using the modified

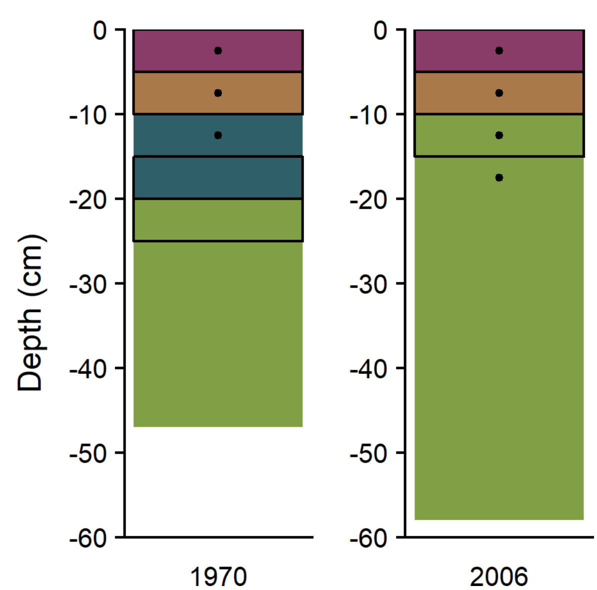

Fig. 1. Model domain for the 1970 and 2006 profiles. The black dots are TDR/observation node depths, and black rectangles mark the location where samples used for the laboratory experiment were taken. The green layers are cut-over peat, and the remaining ones are regenerated moss. (For interpretation of the references to colour in this figure legend, the reader is referred to the web version of this article.)

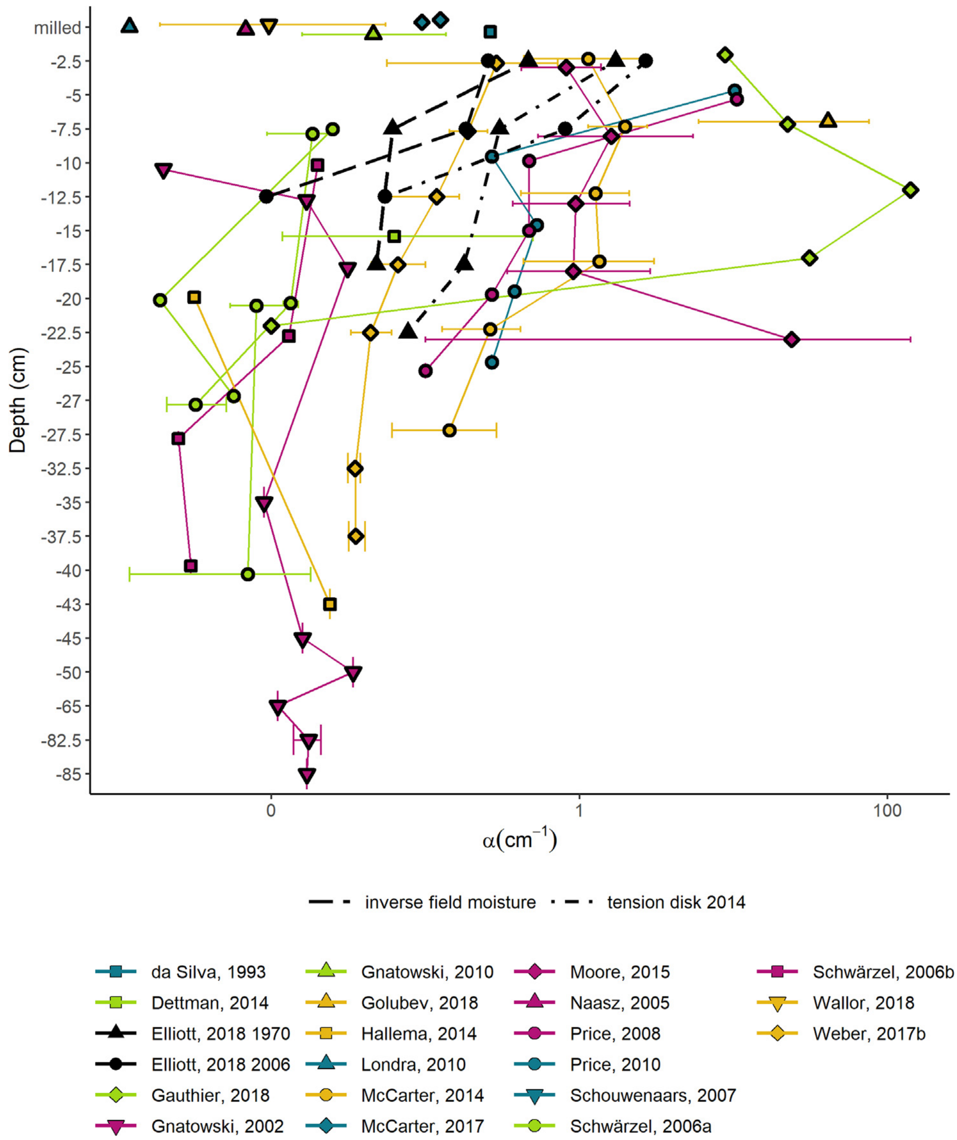

Fig. A1. Combination plot of all literature values for α where the points are the average value, and the error bars are the maximum and minimum values reported.

tension disk method described by McCarter et al. (2017). Following that, bulk density, porosity, and saturated hydraulic conductivity were measured (Taylor and Price, 2015). The depth of samples and TDR probes will define the layers used in later model domains.

2.2. Model setup

HYDRUS-1D was used to numerically simulate soil moisture dynamics in the 2006 and 1970 plots for an 82-day period between May and August 2013, using the parameters estimated from two different techniques described later. The model domains were 0.58 and 0.47 m tall and contained three and four layers for the 2006 and 1970 plots, respectively (Fig. 1). Node spacing was 0.005 m. A variable pressure head was defined as the lower boundary condition. Typically the vertical hydraulic gradient is very low in Northern bogs (Reeve et al., 2000), as such the lower boundary was determined from observed water table measurements. Observed precipitation and estimated potential evaporation from Taylor and Price (2015) were used to characterize the atmospheric boundary condition with surface layer at the top of the domain. Potential evapotranspiration was calculated using the Priestley-Taylor method. The Priestley-Taylor alpha value was set to 1.26 as defined by Priestley and Taylor (1972) and previously used in peatlands by Petrone et al. (2008) and Price (1992). The soil water atmospheric vapour equilibrium (*hCrita*) defines the pressure head at which evaporation capacity is exceeded; evaporation becomes limited when pressure head of the top node reaches *hCritA*, actual evaporation will be less than potential evaporation (Šimůnek et al., 2009). Numerically, *hCritA* is used to increase model stability; it is a lower bound for pressure head to prevent it from changing dramatically when there are small changes in the water content near residual. An *hCritA* of −10 000 cm was used; it is the pressure head at which Thompson and Waddington (2008) and Goetz and Price (2015) suggest soil vapour equilibrium occurs in a cut-over bog at mid-day during the summer and, in a *Sphagnum* profile when the water table is 10 cm below the surface, respectively. Initial soil moisture conditions were determined by linearly interpolating between TDR observations and water table. A spin-up period was not needed because the initial conditions were well defined.

2.3. Determination of soil hydraulic parameters

The van Genuchten-Mualem equation (VGM) is the most widely used soil hydraulic property model within peatland literature (Gauthier et al., 2018; Golubev and Whittington, 2018; McCarter et al., 2017;

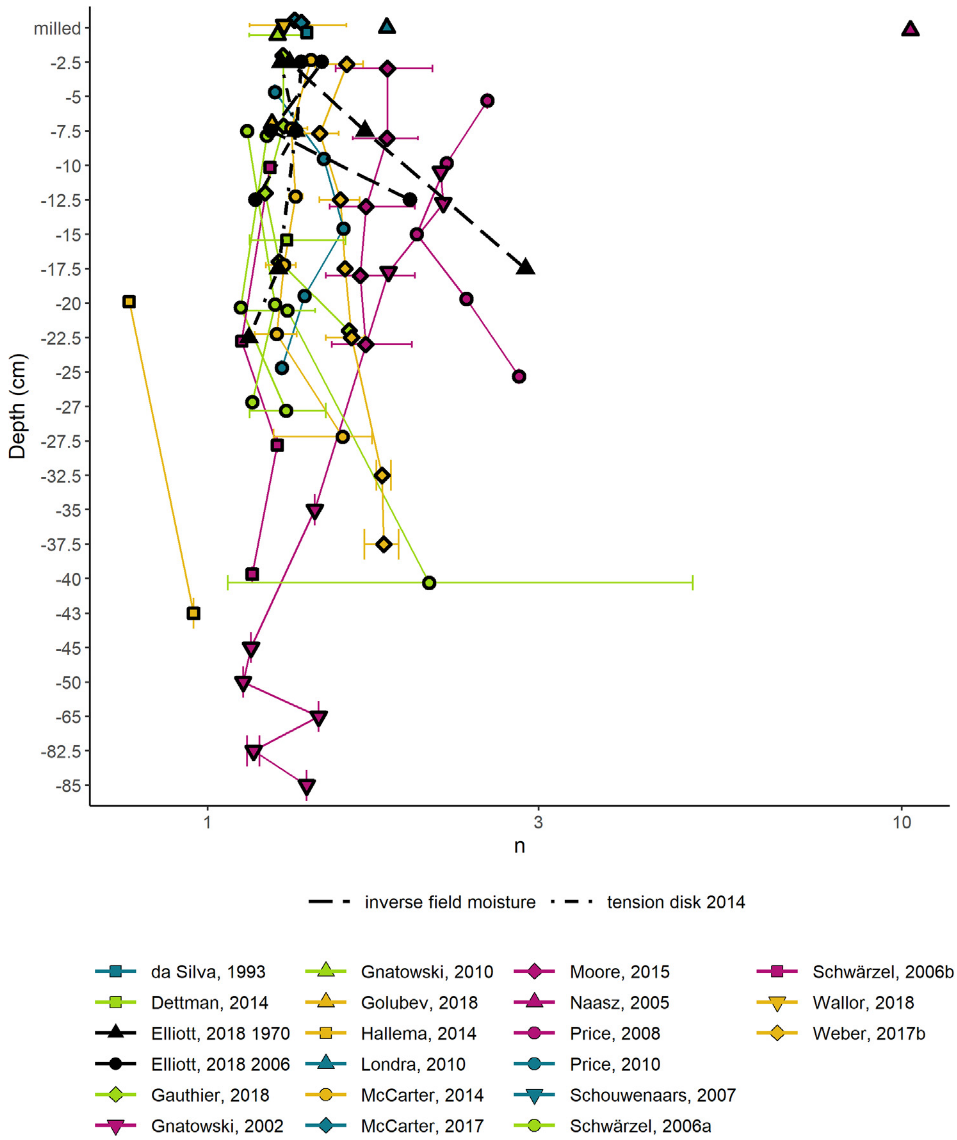

Fig. A2. Combination plot of all literature values for *n*, where the points are the average value, and the error bars are the maximum and minimum values reported.

McCarter and Price, 2014; Moore and Waddington, 2015; Price et al., 2008; Price and Whittington, 2010). The VGM model is defined as:

$$S_e = \frac{1}{(1 + |\alpha\psi|^n)^m} \tag{1}$$

$$S_e = \frac{\theta - \theta_r}{\theta_s - \theta_r} \tag{2}$$

$$K(S_e) = K_s S_e^l (1 - (1 - S_e^{1/m})^m)^2 \tag{3}$$

where S_e is the effective saturation [–], ψ is the pressure head [L], K_s is the saturated hydraulic conductivity [L T^{-1}], and θ, θ_r, and θ_s [cm^3 cm^{-3}] are the water content, residual water content, and saturated water content, respectively. The parameters α [L^{-1}], n, and l are fitting parameters that are related to the inverse of the approximate air-entry pressure, width of the pore size distribution, and the pore-connectivity, respectively. The parameter m is calculated as $1–1/n$.

The VGM parameters (α, n, l and $m = 1–1/n$) were determined using two methods; the first was using RETC software (van Genuchten et al., 1991) based on the hydraulic conductivity and retention data measured by Taylor and Price (2015) in steady-state laboratory experiments for each layer, hereafter referred to SSL parameters. Moreover, any model which used the SSL parameters will be referred to as an SSL model. All measured water content and conductivity measurements at each pressure step were used for fitting unless there was clear evidence of measurement error. To assess for potential measurement error in the laboratory retention experiment error, the water content and hydraulic conductivity observations, for the same pressure step, were plotted on a log–log plot and fit with a linear trend line. Hydraulic conductivity decreases with water content due to less, smaller, and more tortuous pathways; as such, the expected trend is linear or concave-down. If the points trended upward or horizontally with decreasing water content, suggesting that the hydraulic conductivity is maintained or increases for decreasing water content, the points were removed. Approximately 7% of observations were removed. For cut-over peat and moss layers below 15 cm, and all moss layers above 15 cm, θ_r was set to 0.05 and 0.11, respectively; values were based on averages from Weber et al. (2017a). Measured values of total porosity (θ_s) and saturated hydraulic conductivity (K_s) were used (Taylor and Price, 2015). All observations were weighted equally and hydraulic conductivity was log-transformed before fitting, to reduce the numerical difference between water content and hydraulic conductivity values caused by different units. RETC uses Marquardt's maximum neighbour, a local search method, to minimize the weighted least squares objective function. The objective function in RETC simultaneously minimizes the residual sum of squares

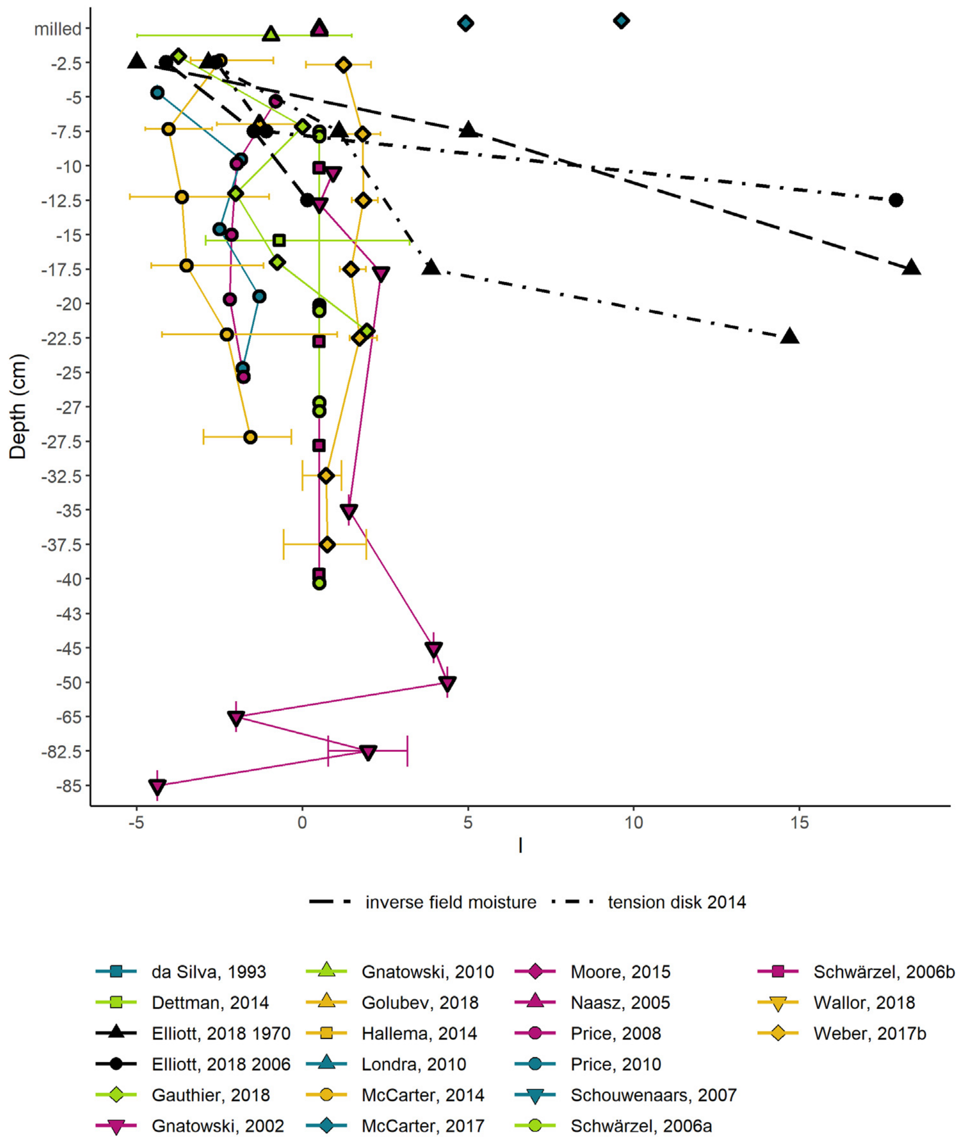

Fig. A3. Combination plot of all literature values for l, where the points are the average value, and the error bars are the maximum and minimum values reported.

error for the retention and hydraulic conductivity curves (van Genuchten et al., 1991). Several authors have noted that local search methods may converge on a local minimum which is not the global minimum (Šimůnek and Hopmans, 2002; van Genuchten et al., 1991). It is recommended to use multiple initial estimates of the parameters (Šimůnek et al., 2012; van Genuchten et al., 1991). As such, initial estimates were manually changed to find a reasonable fit based on a higher relative r^2, smaller relative confidence intervals, and a lower relative objective function value (Tables B.1, B.2). Confidence intervals for SSL parameters were calculated by RETC during the curve fitting process.

The second method was inverse modelling, using HYDRUS-1D v.4.16 (Šimůnek et al., 2009), to fit the soil hydraulic parameters (α, n, l and $m = 1\text{–}1/n$) simultaneously to the observed field soil moisture data from Taylor and Price, (2015). Similar to RETC, HYDRUS uses Marquardt's maximum neighbour method to minimize the weighted least squares objective function of the simulated and observed soil moisture (Šimůnek et al., 2009). However, the objective function only considers water content, and not its relationship with pressure head, see Šimůnek et al. (2009) for more detailed description of the objective function. Confidence intervals were calculated by HYDRUS after parameters were estimated. Inverse modelling was done with data from a transient field experiment, and hereafter the parameters so derived will be referred to as TF parameters. Additionally, models that use TF parameters will be referred to as TF models. Observation nodes were set at depths corresponding to TDR locations in the field. A 20 day subset, between hour 800 and 1280 of the observation period was selected for the calibration period, between hour 800 and 1280 of the observation period, was selected for the calibration period to be used for inverse modelling; the model domain as described below was used. Layers 1–3 in the 1970 profile and layer 1 in the 2006 profile had 480 observations, whereas layers 2 and 3 in the 2006 profile had 446 and 30, respectively. The calibration period was selected to encompass a large range of soil moisture. Initial estimates of the fitting parameters were those determined from SSL parameterization, the bounds of the parameters space, were informed by literature values (Fig. A.1, A.3). In the 1970 profile, no water content observations were made in the peat layer, so that no soil hydraulic properties could be determined for this layer. Therefore, the parameters of the peat layer for 2006 were used. Soil hydraulic parameters from the calibration period were then used to simulate soil moisture for the entire 82-day period. The values used for θ_r, θ_s, and K_s were the same as the SSL model.

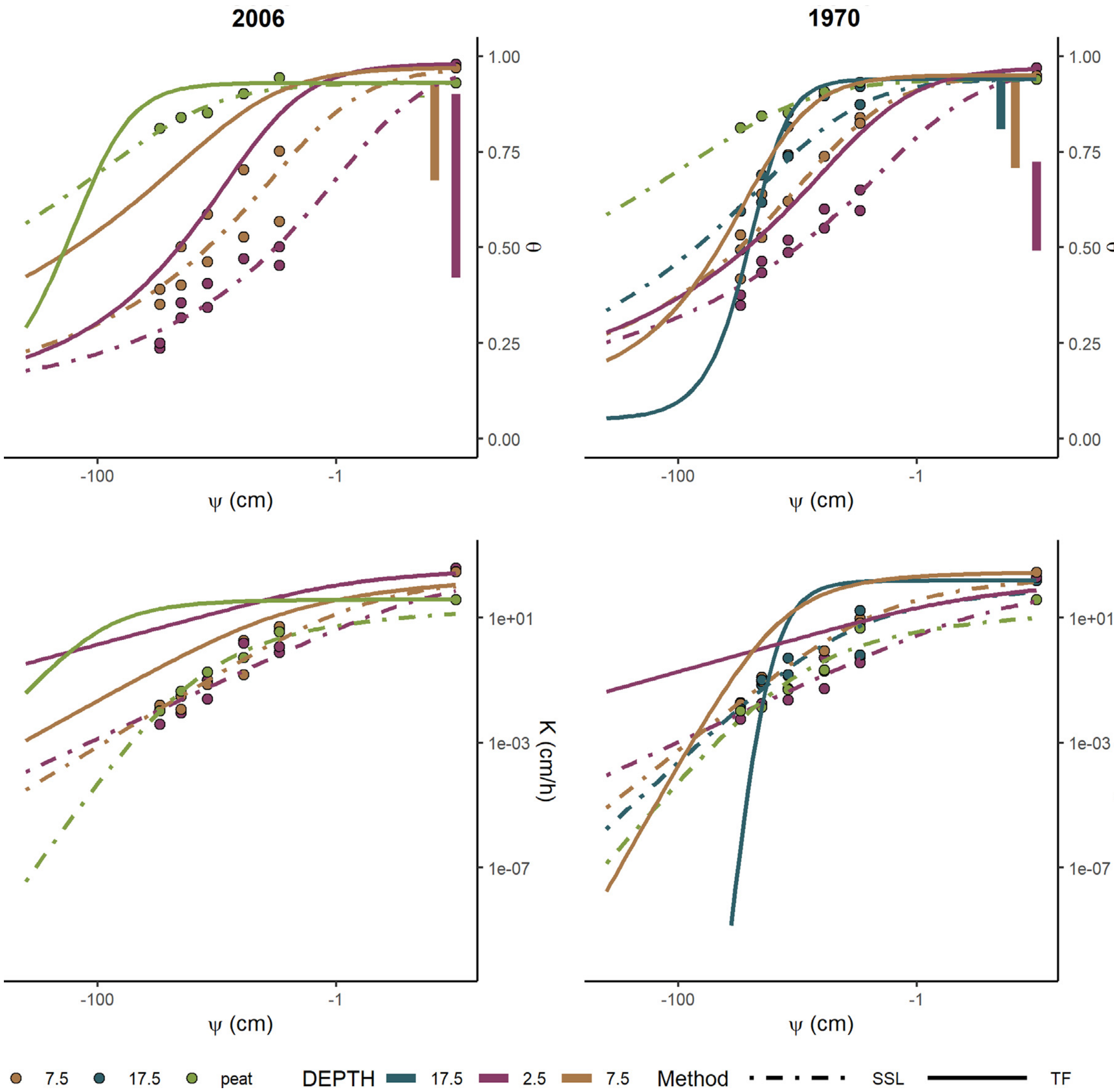

Fig. 2. Retention curves (Top) and hydraulic conductivity curves (Bottom) for SSL and TF parameters for the laboratory observations and the field observations, respectively. Points represent observations from the SSL experiment. The vertical lines denote the water content range of the calibration period used for the TF parameterization.

Table 1
Model parameters and the 95% confidence interval.

Method	Plot	Depth	α (cm^{-1})	α CI	n	n CI	l	l CI
TF	1970	2.5	0.47	0.04	1.31	0.01	−5	5.92
TF	1970	7.5	0.06	0.00	1.9	0.05	5	51.5
TF	1970	17.5	0.05	0.00	2.87	0.23	18.38	84.8
TF	2006	2.5	0.26	0.02	1.46	0.02	−4.11	49.92
TF	2006	7.5	0.18	0.02	1.23	0.02	−1.46	11.09
TF	2006	peat	0.93	0.05	1.96	7.84	0.16	141.79
SSL	1970	2.5	1.71	0.91	1.28	0.05	−2.85	1.7
SSL	1970	7.5	0.3	0.12	1.34	0.08	1.1	2
SSL	1970	17.5	0.18	0.11	1.27	0.11	3.87	5.45
SSL	1970	peat	0.08	0.04	1.15	0.06	14.7	15.1
SSL	2006	2.5	2.7	2.2	1.37	0.1	−2.61	1.7
SSL	2006	7.5	0.81	0.6	1.34	0.12	−1.08	2.57
SSL	2006	peat	0.05	0.01	1.17	0.04	17.92	8.38
ALT	1970	2.5	0.28	0.06	1.57	0.08	1.18	1.49
ALT	1970	7.5	0.17	0.04	1.41	0.09	0.03	35.03
ALT	1970	17.5	0.08	0.02	1.52	0.26	2.53	141.67
ALT	2006	2.5	0.26	0.04	1.55	0.06	1.16	1.36
ALT	2006	7.5	0.16	0.03	1.38	0.05	0.01	15.25
ALT	2006	peat	0.01	0.03	1.21	2.03	1.87	2774.77

2.4. Model performance

Several error metrics were calculated to assess whether the SSL or TF parameterization was better at representing the soil moisture observed in the 1970 and 2006 profiles. Calculations were done using simulated and observed soil moisture for 62 days of the 82-day observation period to exclude the calibration period. Model performance was assessed using five statistical metrics: mean absolute error (MAE), root mean square error (RMSE), mean bias error (ME), Nash-Sutcliffe efficiency (NSE), and modified Kling-Gupta efficiency (KGE'), such that:

$$MAE = \frac{1}{n'} * \sum |X_s - X_o| \tag{4}$$

$$RMSE = \sqrt{\frac{1}{n'} * \sum (X_s - X_o)^2} \tag{5}$$

$$ME = \frac{\sum X_s - X_o}{n'} \tag{6}$$

$$NSE = 1 - \frac{\sum (X_o - X_s)^2}{\sum (X_o - \bar{X}_o)^2} \tag{7}$$

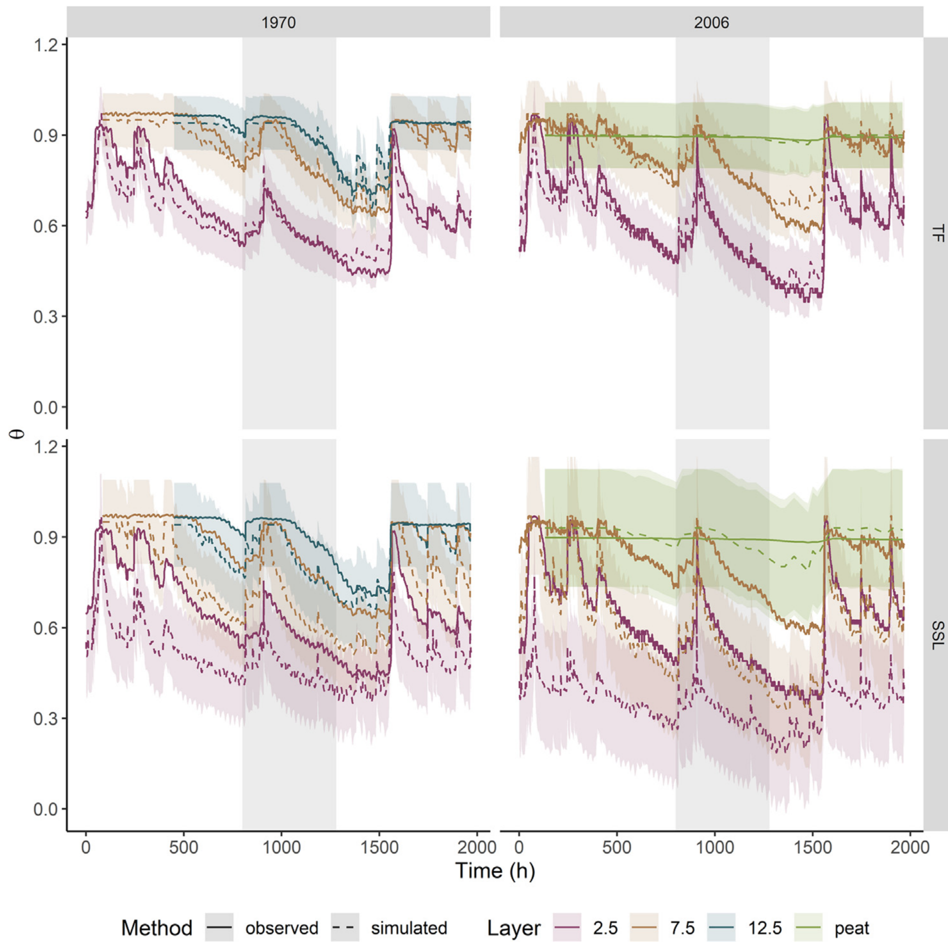

Fig. 3. Time series of observed and simulated soil moisture for all models. The shaded grey area denotes the calibration period. The shaded area around the simulated soil represents the 95% prediction interval. Both observed and simulated nodes in the peat layer behaved the same; the lower one (17.5 cm depth) was removed for simplicity.

Table 2
Model error statistics.

Method	Plot	MAE	ME	RMSE	NSE	KGE'	Pearson r
SSL	2006	0.25	−0.25	0.27	−1.4	0.23	0.82
SSL	1970	0.12	−0.11	0.14	0.24	0.63	0.90
TF	2006	0.04	−0.01	0.06	0.89	0.89	0.95
TF	1970	0.04	−0.02	0.05	0.91	0.93	0.96
ALT	2006	0.04	0.00	0.06	0.89	0.83	0.95
ALT	1970	0.06	−0.01	0.07	0.79	0.77	0.90

$$KGE' = 1 - \sqrt{\left(\frac{Cov_{so}}{\sigma_s * \sigma_o} - 1\right)^2 + \left(\frac{\sigma_s/\bar{X}_s}{\sigma_o/\bar{X}_o} - 1\right)^2 + \left(\frac{\bar{X}_s}{\bar{X}_o} - 1\right)^2} \tag{8}$$

Table B.1
Initial parameters for curve fitting in RETC and inverse modeling in Hydrus-1D.

Method	Plot	Depth	θ_r (cm^3 cm^{-3})	θ_s (cm^3 cm^{-3})	α (cm^{-1})	n	K_s (cm d^{-1})	l
SSL	1970	2.5	0.11	0.97	0.5	1.56	4699	0.5
SSL	1970	7.5	0.11	0.95	0.04	1.56	6959	0.5
SSL	1970	17.5	0.05	0.94	0.04	1.56	370	0.5
SSL	197	peat	0.05	0.94	0.04	1.56	913	20
SSL	2006	2.5	0.11	0.98	2	1.56	9397	0.5
SSL	2006	7.5	0.11	0.97	20	1.1	7310	−6
SSL	2006	peat	0.05	0.93	0.04	1.56	910	0.5
TF	1970	2.5	0.11	0.97	1.71	1.28	4699	−2.85
TF	1970	7.5	0.11	0.95	0.3	1.34	6959	1.1
TF	1970	12.5	0.05	0.94	0.18	1.27	3703	3.87
TF	1970	peat	0.05	0.9	0.01	1.96	912	0.16
TF	2006	2.5	0.11	0.98	2.7	1.37	9397	−2.61
TF	2006	7.5	0.11	0.97	1.5	1.34	7310	−1.08
TF	2006	peat	0.05	0.9	0.01	1.17	909	17.92
ALT	1970	2.5	0.11	0.97	0.29	1.6	4699	1.24
ALT	1970	7.5	0.11	0.95	0.19	1.45	6959	1.82
ALT	1970	12.5	0.05	0.94	0.09	1.57	3703	1.65
ALT	1970	peat	0.05	0.9	0.01	1.21	912	1.87
ALT	2006	2.5	0.11	0.98	0.29	1.59	9397	1.24
ALT	2006	7.5	0.11	0.97	0.19	1.45	7310	1.82
ALT	2006	peat	0.05	0.9	0.01	1.17	909	17.92

where *n'* is the number of observed and simulated water content pairs, and X, $\bar{X}$, and σ are the samples, means and standard deviations, respectively, for the corresponding subscript, simulated (s), and observed (o) data. Cov_{so} is the covariance between the simulated and the observed. MAE is a measure of average error magnitude, while RMSE is a more conservative quantification of error where larger errors have more influence. The ME indicates whether the simulations tends to over (positive) or under (negative) predict the observations and is expressed as in original units. Lower values of MAE, RMSE, and ME indicate a better fit. The NSE is a measures of overall model performance that compares the performance of the simulation to the performance of the mean (Nash and Sutcliffe, 1970). KGE' is a multi-objective approach that combines correlation, simulated-observed mean ratio, and variability (Kling et al., 2012). Ideal values of NSE and KGE' are unity and have no lower limit; simulations with values above 0.7 were considered acceptable. The threshold of 0.7 was selected based on what is

Table B2
The upper and lower bounds of the parameter space used during inverse simulation in Hydrus for all layers.

	α (cm^{-1})	n	l
upper bound	1000	3	5[a]
lower bound	0	1.001	−5

[a] For the peat layer l had an upper bound of 20.

commonly used in the literature (Crochemore et al., 2015; Moriasi et al., 2015), for further discussion on the difficulty defining error metrics see Gupta et al. (2012). All error metrics were computed in R 3.5.0 (R Core Team, 2018) with the hydroGOF package (Zambrano-Bigiarini, 2017). A residual plot was created to assess the appropriateness of the unimodal VGM model. Model performance was only calculated for the validation period.

2.5. Sensitivity analysis

A one at a time sensitivity analysis was done to assess which parameters had the greatest impact on model accuracy by individually increasing and decreasing α, n, and l by 10 steps, incremented by log (0.15), 0.03, and 0.5, respectively. Intervals were selected to represent a large portion of the parameter space presented by literature values (Figs. A.1, A.2, A.3). The sensitivity analysis was done on both profiles and fitting methods for all fitting parameters on each layer. Furthermore, a sensitivity analysis on the evaporative boundary condition was done during inverse modelling to assess how a different Priestley-Taylor alpha value would influence parameter estimation. The Priestly-Taylor alpha value was increased and decreased by 0.1, 0.2, 0.3, and 0.4 to represent a range of values that have previously been used in bogs (Humphreys et al., 2006; Petrone et al., 2004; Price et al., 1998). The TF parameterization was repeated with an alternate set of initial estimates (ALT) to assess how final parameter estimates would change and the impact it would have on the overall model fit. The alternate estimates came from the average value of their equivalent depth form Weber et al. (2017a); initial estimates of the 1970 and 2006 peat layers were from the 37.5 cm layer.

3. Results

3.1. Parameter estimation

The parameterization using SSL data produced curves that agreed well with the laboratory observations. All SSL curves had an r^2 above 0.8 with the exception of the 1970 – 17.5 layer, which had an r^2 of 0.73. With decreasing pressure head the water content decreased sharply in the moss layers; whereas the water content in the peat layers decreased gradually (Fig. 2). Curves produced from TF data (Fig. 2) do not have comparable points against which to visually judge the fit. However, the 2.5 and 7.5 cm retention curves from TF model showed that drainage would start at a lower pressure head than the SSL curves. Similarly, the lowest layers in the TF models (1970 – 17.5 and 2006 – 12.5) started to drain at a higher pressure head and drained substantially quicker than their SSL model counterpart (Fig. 2). The hydraulic conductivity curves from the TF parameterization were higher than those of the SSL parameterization, however the 7.5 and 17.5 cm layers for the 1970 profile decreased sharply around – 10 cm of pressure head (Fig. 2). The estimates of the VGM parameters for the 1970 and 2006 SSL and TF model parameters differed (Table 1) despite both RETC and HYDRUS reporting a good fit during direct curve fitting and inverse modelling, respectively. The parameter α decreased with depth for both curve fitting methods and profiles (Table 1). Additionally, parameterization with TF data yielded α values that had smaller confidence intervals ($< = 0.05$ cm^{-1}), as such they were well defined. SSL values of n were higher in moss layers (~1.32) than cut-over peat (~1.16), whereas from the trend for TF modelling was the opposite. The 1970 and 2006 SSL, and 2006 TF parameterizations had l values that increased with depth (−4.11 to 0.16); no trends were present for the 1970 TF parameters. The 2006 and 1970 SSL peat layers and 1970 TF 17.5 layer all had very large l values (> 5). Based on the confidence intervals, parameter n was generally well defined for all fitting methods (0.01–0.23), whereas l values fit with the TF data, or the lower layers fit with SSL data were poorly defined (5.92–141.79). An exception to the trends presented for the confidence intervals of α and n was the 2006 TF peat layer, both of which were poorly defined.

3.2. Model performance

Fig. 3 depicts simulated and observed soil moisture over the simulated period for the 1970 and 2006 profiles fit with both methods. Visually, the TF model fit better than the SSL model, with the poorest fit

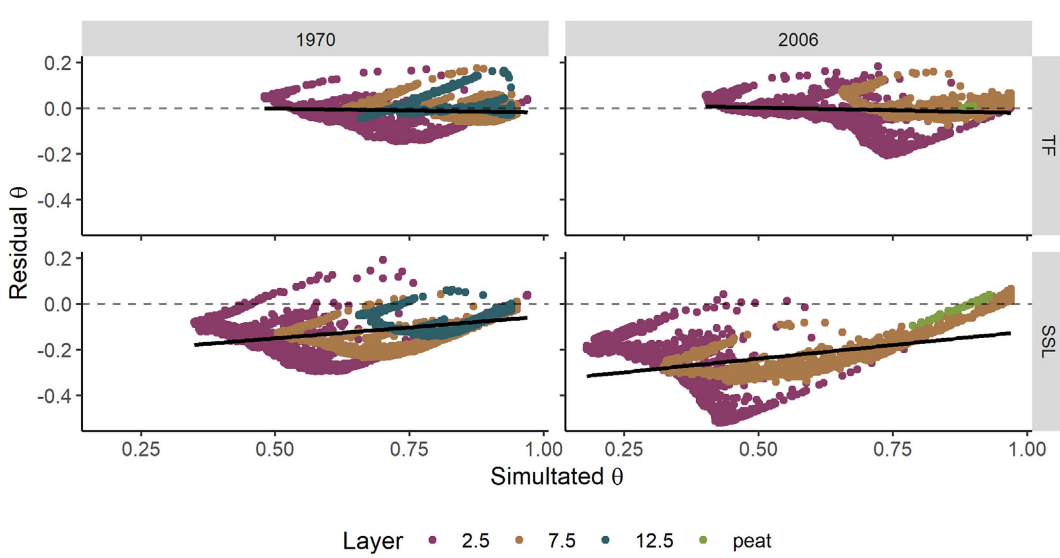

Fig. 4. Residual plot of the modeled field scale soil moisture. The most easily observed looped pattern is when the soil moisture increases from the lowest simulated soil moisture and rises above the other observations; this corresponds with the large wetting event around hour 1500.

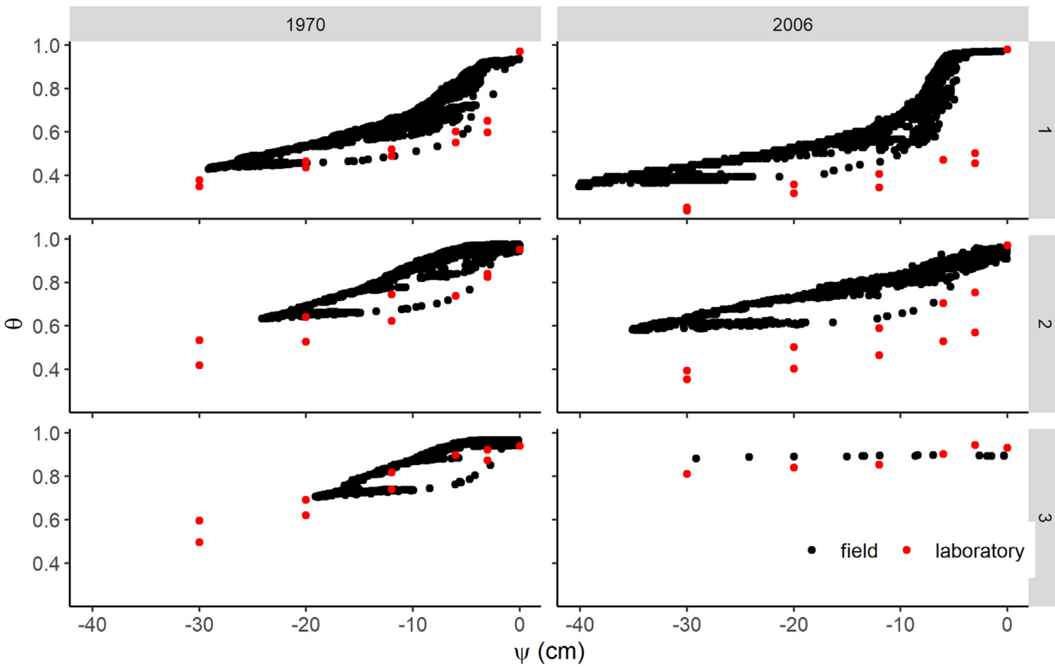

Fig. 5. Observed SSL and assumed TF θ-ψ relationships. Superposition of laboratory retention curves on field retention curves for each layer. Pressure of the field observations is assumed from the depth of the water table below the soil moisture observation point. Layer 3 of the 2006 probe has fewer observed field data because soil moisture was recorded manually and not logged.

in the top two layers of each profile. Notably, the peat layer of the 2006 SSL model started to drain (hours 1000–1500), yet it did not in the TF simulation. The TF simulations visually matched the observed much better; however, both profiles underestimate soil moisture during the initial period with large soil moisture fluctuations and overestimate during the driest period.

The mass balance error calculated by HYDRUS was less than 1% for all simulations. Within each model, the RMSE and MAE were similar; as such there were no large outliers in model, (Table 2). As mentioned earlier, the SSL parameters resulted in simulations that poorly matched the observed data. The RMSE of the TF models was similar to the threshold of probe error, a water content of ~0.05. The SSL models had large negative ME and indicates bias in the model; whereas, the ME of TF models was approximately 0, indicating no bias. The poor performance of the SSL models is reflected in low NSE and KGE'; although both metrics were below 0.7, the KGE' is notably higher than the NSE. Conversely the NSE and KGE' scores for the TF models were both above 0.7. Visually, the residual plots were not randomly distributed (Fig. 4); suggesting that the model may not account for all processes or properties (Daniel and Woods, 1980). The 2006 profiles had a distinct peak in the 2.5 cm layer. All profiles had a distinct pattern in the residuals which resembles a hysteresis (Fig. 4).

The forward simulation for both profiles and fitting methods were most sensitive to changes in α and least sensitive to l (Fig. 6). Adjusting α parameters of the upper layers in the SSL models and the 1970 TF model reduced the RMSE by up to 0.01 and 0.075 from the original parameterization. Changes in the parameter l increased or decreased the RMSE of the TF forward simulation by less than 0.01. Additionally, the estimates of the soil hydraulic parameters exhibited little sensitivity to the choice of the Priestley-Taylor alpha within the range of 0.86–1.66 (Fig. 7). Changes in α for the 2006 profile, for a Priestley-Taylor alpha of 0.96 and 1.66, are likely an artefact of the minimization process during inverse modelling.

4. Discussion

4.1. The influence of fitting method on parameters

Based on model performance, parameters fitted using empirical curves from laboratory experiments (SSL parameters) were not able to simulate soil moisture in the field, despite good agreement with laboratory curves. The majority of observed soil moisture values in all moss layers occurred above the highest moisture measurement used when fitting SSL data in RETC (Fig. 5). As such, the SSL model under predicted soil moisture, which is reflected in the low ME and the large number of negative residuals (Fig. 4). It is possible that the laboratory parameters poorly represent field conditions because a laboratory sample may drain beyond the first pressure step of hysteretic effects on soil moisture when preparing the sample for the experiment such that the soil moisture is no longer on the main drying curve for the first pressure step, but between the main drying and wetting curve, on a scanning curve. A similar discrepancy was proposed by Schelle et al. (2013) when comparing retention curves from evaporation experiments and suction plates in sandy soils. When laboratory observations of the θ-ψ curve are overlain on θ-ψ curve from the field (where pressure head is estimated from water table depth), generally laboratory observations align with the wetting/scanning curves of the estimated field retention curve (Fig. 5). This suggests that the modified retention disk method captured a scanning curve far removed from the main drying curve. It would not be unreasonable to assume similar limitations using pressure cells (e.g. Moore et al., 2015). Although pressure head in the field was not measured, it can be estimated from the water table level as a linear 1:1 decrease with height above the water table. Pressure head may deviate from the 1:1 equilibrium line by increasing and decreasing during precipitation and evaporation, respectively. During precipitation field observations which represent wetting would shift towards that the observed laboratory observation whereas those representing drying would further deviate from laboratory observations. Alternatively, the samples taken may not be representative of field conditions due to the small sample size. However, other studies that parameterized α using data from the original and modified retention disk experiment had VGM

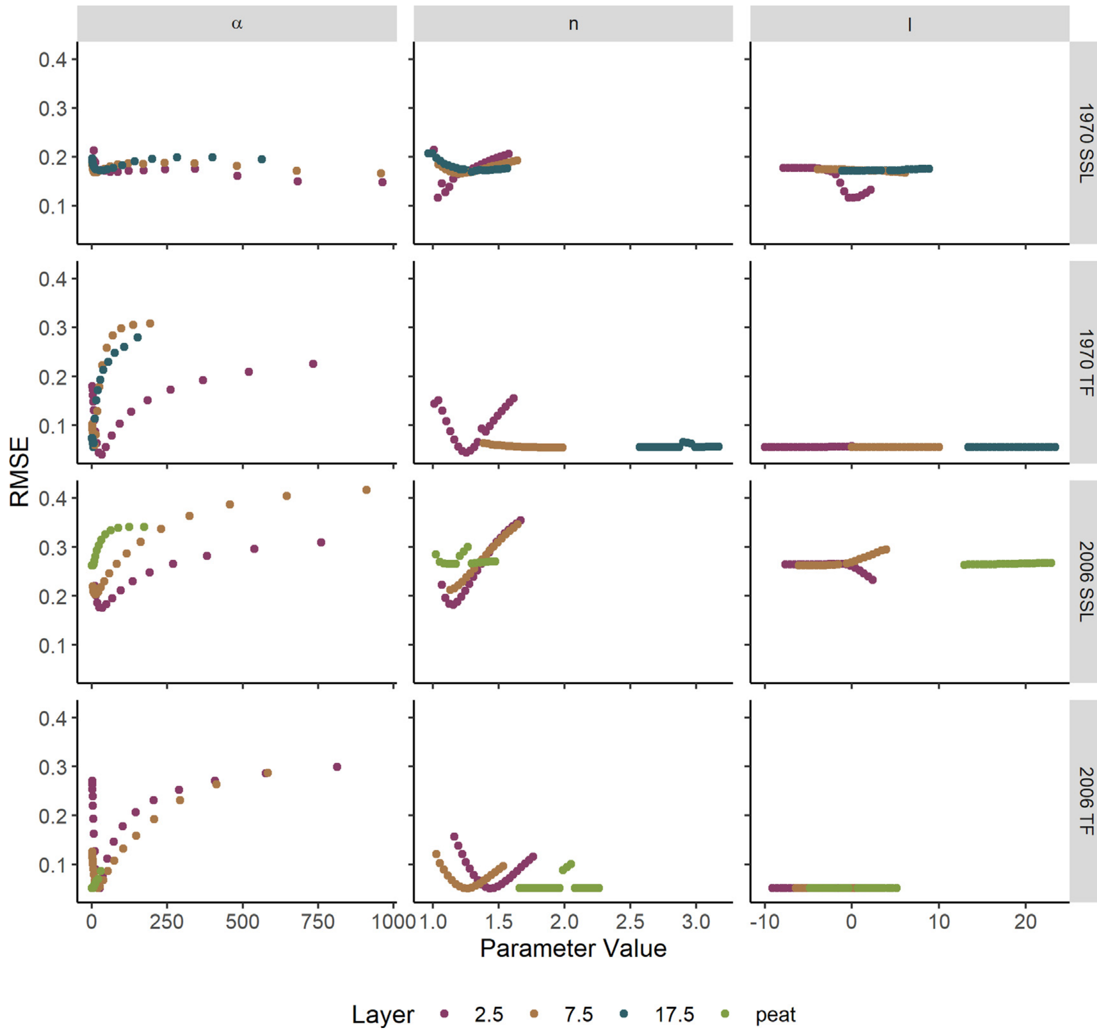

Fig. 6. Sensitivity Analysis of all profiles and methods for all fit parameters. Trends in α were stable as such it was limited to values below 1000 for clarity.

parameter estimates similar to this study (Gauthier et al., 2018; Golubev and Whittington, 2018; McCarter and Price, 2015; Price et al., 2008; Price and Whittington, 2010).

The α parameter consistently decreased with depth for both fitting methods and profiles, which matches virtually all literature trends (Fig. A.1; Moore et al., 2015). Although α is strictly a fitting parameter (Peters et al., 2011), it approximates the inverse of the air-entry pressure; larger values result in drainage occurring at pressures closer to zero. Decomposition and compression decreases the number of large pores and increase bulk density, which has been found to be inversely related to α. As such, a smaller α value is expected with depth, especially in the older cutover peat, because it is highly decomposed and much denser (Bloemen, 1983; Moore et al., 2015; Sherwood et al., 2013; Weiss et al., 1998). Additionally, the α parameter was notably different depending on the method of parameterization. The α values from SSL parameterization were higher than those from TF parameterization because soil moisture observations in the SSL experiment were lower than those of TF experiment at equivalent pressure head (Fig. 5); however, they were well within the range of literature values (Fig. A.1). This is due largely to the difference in water content at equivalent pressure head in the data used for parameterization between the two methods (Fig. 5). If other steady-state experiments reported in the literature were also subject to large drainage after saturation and before the experiment began, α may be overestimated because the curve was fit to observations akin to a scanning curve rather than the main drying curve. Although the parameter estimations were not unreasonable, the SSL α values had large confidence intervals (Table 1). Conversely, the moisture content during the TF calibration period included saturation for all layers with the exception of 1970 – 2.5, which would suggest that α should be more reliable. The confidence intervals for all TF layers were very small, suggesting that the parameters are more identifiable. The 2006 TF peat layer (12.5 cm layer) was the exception; this is most likely due to the extremely narrow range of soil moisture that it experienced. The water table was on average 14 and 17 cm below the surface with a standard deviation of 6.7 and 8.9 cm for the 1970 and 2006 plots, respectively. As such the large ME for SSL models is most likely due to drainage occurring close to zero pressure head. The superior fit to TF experiments for the parameter α was further demonstrated during rain events (Fig. 3). The simulated soil moisture in the TF models is generally maintained after a precipitation event and matches the observed drying, whereas the simulation with SSL derived parameters shows ad immediate desaturation after precipitation stops (Fig. 3). The quick drainage associated with α, after precipitation, in the SSL models is likely what contributes to the low ME values. Model fit has been found to be most sensitive to α in this study (Fig. 6) and others (Kettridge et al., 2016; Weiss et al., 1998); as such accurate characterization of α is important.

Unlike α, the parameter n was very well defined for the SSL models (Fig. 6); this is most likely due to the majority of the laboratory observations being within the moisture range where drainage occurs. Assuming that the SSL experiment captured a scanning curve, rather than the main drying curve, there is reason to believe that the

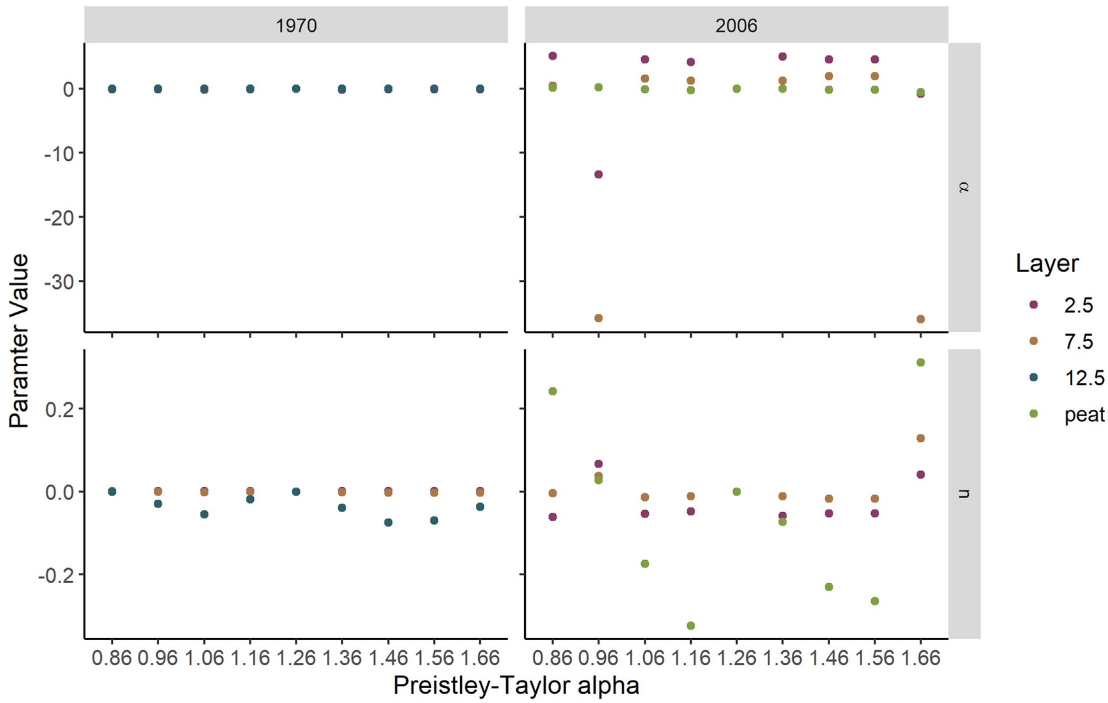

Fig. 7. Sensitivity analysis of parameters during inverse simulation to the transient field data. The parameter *l* was excluded because the data range was not sufficient to adequately define it.

parameter *n* should still be reasonably accurate. Implementations of models that include hysteresis assume that *n* is equal for the wetting and drying branch of the retention curve (Šimůnek et al., 2009). Thus, it is reasonable to extend the assumption, of *n* being the same during wetting and drying conditions, to include scanning curves as well. The appropriate rate of drainage is reflected in the high r^2 for the RETC models; 0.9 and 0.82 for 1970 and 2006, respectively. The parameter *n* is associated with the range of the pore size distribution; larger values represent a narrower pore-size distribution, which results in rapid drainage after air-entry (Peters et al., 2011). Literature values for *n* from direct curve fitting and inverse modelling generally decreased with depth; values from both SSL parameterizations were consistent with the trends (Fig. A.1). Despite the TF model fitting well and values within range of the literature, it produced *n* values that were inconsistent with depth, likely due to an insufficient soil moisture range during calibration. The function of the parameter *l* in the VGM is to control how quickly hydraulic conductivity decreases with pressure beyond air-entry (Mualem, 1976; Peters et al., 2011), where negative values result in a more gradual decrease in hydraulic conductivity (Gnatowski et al., 2010). The parameter *l* is related to pore-connectivity and tortuosity under unsaturated conditions, but is widely believed to have no meaning (Ghanbarian et al., 2013; Peters et al., 2011; Schaap and Leij, 2000). The forward simulations were not sensitive to changes in *l*, especially in lower layers, which was generally a poorly defined parameter (Fig. 6). In particular, SSL estimates for 1970 and 2006 peat layers and the 17.5 cm layer form the 1970 profile were far beyond what has previously been reported in the literature (−5 to 5; Fig. A.1). It is likely that the range of measurements does not contain the required information to accurately predict *l*. Additionally, the majority of literature values from direct curve fitting were all negative (Fig. A.3), notably foundational work done by Price et al. (2008) and McCarter and Price (2014). Dettmann et al. (2014) suggests that *l* is not a sensitive parameter during saturated conditions where the pressure head of a *Sphagnum* moss profile is above −200 cm. The range of pressure head experienced during the calibration period was greater than the −200 cm threshold, which supports the idea that inadequate information was available. As such, *l* should simply be considered a fitting parameter, regardless if it is positive or negative. Given its low sensitivity, it would be reasonable to fix *l* to reduce complexity of direct curve fitting or inverse modelling.

4.2. Did the model actually fit?

The parameters fit with data from an SSL experiment were not able to simulate the observed soil moisture well at any depth (Fig. 3). Furthermore, the RMSE, MAE, and ME of each SSL model is approximately the same within each profile, which suggests that the simulation of soil moisture was poorly predicted systematically (Table 2). As in the study by Schwärzel et al. (2006a), the SSL models under-predict soil moisture, which is most likely a consequence of the high *α* parameter values. Furthermore, *α* was found to be a sensitive parameter in this study, and by Weiss et al. (1998). Discussion by Schelle et al. (2013) and Golubev (2018) suggest that samples may not be fully saturated for all steady-state laboratory experiments (tension disk and pressure cell) because drainage may occur before the sample is in the measurement device. This is supported by the difference between *α* estimates fit to steady-state and transient experiments (Fig. A.1).

The RMSE of the TF models matched the error threshold of the TDR probes (~0.05), which was substantially better than the SSL models. Inverse modelling of field lysimeter experiments conducted by Schwärzel et al. (2006a) also estimated parameters that were better able to simulate field observations of soil moisture than parameters from laboratory derived retention curves. Their parameters from inverse modelling of transient laboratory (TL) evaporation experiments also performed substantially better than steady-state experiments (TF > TL ≫ SSL) (Schwärzel et al., 2006a). The TF model used here did not perform well during rain events (e.g., hours 1400–1600) and under-predicted soil moisture; although Schwärzel et al. (2006b) had the opposite problem, soil moisture was over-estimated. It was possible that this could be due to the difference in estimates of *α*, which reflects an air-entry pressure that is not representative of wetting and drying processes. Parameters from inverse modelling were also unable to describe soil moisture beyond the calibration range; Schwärzel et al. (2006a) reported similar difficulties predicting beyond the calibration.

The observed shortfalls may be a result of missing soil hydraulic processes or properties, as is suggested by non- random distribution of the residuals, distinct patterns were observed (Fig. 4). The TF simulation over-estimate moisture in the dry range and under estimated moisture near saturation. Furthermore, the distribution of points where soil moisture was over estimated (below the dashed line) appeared to follow a looped pattern, in a clockwise direction (Fig. 4). Additional process and properties, such as hysteresis and dual porosity, respectively, may need to be accounted for. Hayward and Clymo (1982) have remarked on the dramatic effect that hysteresis can have on water content; since then several authors have observed it when building retention curves from laboratory experiments (da Silva et al., 1993; Londra, 2010; McCarter and Price, 2014; Naasz et al., 2005; Price and Whittington, 2010). Likewise, Taylor and Price (2015) observed hysteresis with the dataset used for this study when plotting soil moisture in the top 5 cm against water table depth. If hysteresis is a process that is not accounted for within the calibration period, then α would represent an aggregate of the wetting and drying cycles rather than the actual main drying curve.

Hayward and Clymo (1982) highlight two major pore systems: the matrix created by overlapping branches, and the pores of individual cells. As such, the assumption of unimodality of the pore-size distribution in the VGM would be violated, as suggested by Price et al. (2008). Dettmann et al. (2014) found evidence of a second pore domain at ~ -400 cm of pressure, which coincides with the range of pressures at which hyaline cells drain (Lewis, 1988). Pressures observed in this study are insufficient to drain hyaline cells; which would suggest a single porosity model should suffice. Alternatively, Weber et al. (2017b) found evidence of a triple porosity model where the first pore domain was encompassed by a pressure head between 0 and -10 cm. The non-normal distribution of the residual from the 2006 TF model, notably the 2.5 cm layer, could suggest that a dual porosity model may better describe the soil water retention curve (Fig. 4). Further investigation is required. The methods used for the SSL experiment did not produce a dataset which was granular enough to assess bimodality near saturation.

4.3. Limitations and error

Parameterization from SSL and TF modeling experiments can be restricted by a limited observation range to which they were fit, compromising realism and accuracy (Šimůnek et al., 2009; van Genuchten et al., 1991). The narrow range of θ-ψ observation was a major limitation to confidently estimating parameters in this study. Aside from potential methodological errors in steady -state laboratory experiments, the pressure head is limited to a range where moss is not stressed (Hayward and Clymo, 1982). A restricted pressure head range is not an issue for managed systems (e.g. *Sphagnum* fibre farming), however, it would be important for predictions where the pressure head range is unknown (e.g. drought). Similarly, curve fitting in the lower layers of the TF models suffered from being fit to a small range of observations and was reflected in the increasing magnitude of the confidence intervals with depth. Laboratory evaporation experiments may be best suited to build retention curves because large portions (Dettmann et al., 2014), or the entire moisture range can be captured (Schelle et al., 2013; Weber et al., 2017b).

Curve fitting using RETC and HYDRUS is limited by the estimation algorithm, it is recommended that several initial conditions are used to properly estimate parameters (Šimůnek et al., 2009; van Genuchten et al., 1991). A thorough exploration of the impact of initial conditions was not done due to the complexity associated with estimating parameters for a multi-layered system. Daniel and Woods (1980) recommend when using a local solver, initial parameter estimates should approximate the real value, as such different initial conditions based on newly and previously estimated parameters were compared. Two sets of initial estimates were assessed, the first were the parameter estimates from RETC, the second were from inverse modelling of evaporation experiments (ALT) by Weber et al. (2017b). Estimates of α remained similar between the ALT and TF parameterizations; however, ALT values had more uncertainty (Table 1). Additionally, the estimates of n from the ALT model were more realistic and decreased with depth, as is expected with an increase in bulk density (Moore et al., 2015; Sherwood et al., 2013). The largest difference was in the pore connectivity parameter l. ALT parameters were all positive and had a much smaller range, notably the 1970 profile. Despite the ALT parameters being more reasonable than the TF parameters, the confidence intervals were equally large. The MAE, ME, RMSE, NSE, and KGE' of the 2006 ALT model were virtually identical to the 2006 TF model. Alternatively, the error metrics of the 1970 ALT model showed that it performed worse than 1970 TF model (Table 2). Multiple sets of parameter sets which result in an acceptable fit supports the idea that the model is ill-posed, as is suggested by Šimůnek et al. (2009) when simultaneously fitting 15 parameters. In the absence of additional evidence several parameter sets may produce an acceptable prediction (Beven, 2006, 1993); as such, model predictions would be acceptable within the calibrated range. Using global search methods would better be able to explore the parameter space (e.g. Weber et al., 2017a; b).

5. Conclusion

The objective of this study was to determine which method led to a parameter set which most accurately described the soil moisture dynamics at the field-scale, when determined by direct curve fitting to SSL experiments or inverse modelling to TF observations. SSL parameters consistently underestimated soil moisture in the field, despite being in agreement with literature values. Parameters estimated, using inverse modelling, were adequately able to describe field-scale soil moisture; however, the fit was generally poor when simulated soil moisture exceeded the observed range used for calibration. As such the use of parameters determined with TF simulations would be more useful for predicting soil moisture in managed peatlands where extreme conditions are not allowed to go beyond the calibration, such as *Sphagnum* fibre farming. In order to predict soil moisture in a more robust manner a different model that accounts for other processes and properties may be required. The non-random distribution of the residuals alludes to other processes and properties that should be considered, such as hysteresis and multiple pore domains. Parameterization of peatland soil water retention, with the goal of predicting soil moisture under a large variety of condition, should be done with deliberate laboratory or field evaporation experiments where a large range of soil moisture can be observed. However, if the intended use of the model is for managing *Sphagnum* fibre farming operations or other scenarios where the water table is maintained near the surface, a limited calibration, like the one used in this study, is acceptable.

James Elliott and Jonathan Price conceptualized the goals of the project; James Elliott developed the methodology, conducted the investigation and formal analysis; Jonathan Price provided the data set which James Elliott curated; James Elliott wrote the original draft and created the visualization; James Elliott and Jonathan Price reviewed and edited the manuscript; Jonathan Price supervised the project and acquired funding.

Declaration of Competing Interest

The authors declare that they have no known competing financial interests or personal relationships that could have appeared to influence the work reported in this paper.

Acknowledgments

We would like to acknowledge financial support from a NSERC Collaborative Research and Development grant (CRDPJ 437463 – 12) and the Canadian Sphagnum Peat Moss Association and its members. We would also like to thank Owen Sutton for his help in interpreting modelling outputs. Lastly, we would like to thank the reviewers for their comments which helped improve the clarity of the paper

Appendix A. Supplementary data

Supplementary data to this article can be found online at https://doi.org/10.1016/j.jhydrol.2019.124489.

References

Beven, K., 2006. A manifesto for the equifinality thesis 320, 18–36. https://doi.org/10.1016/j.jhydrol.2005.07.007.

Beven, K., 1993. Prophecy, reality and uncertainty in distributed hydrological modelling. Adv. Water Resour. 16, 41–51. https://doi.org/10.1016/0309-1708(93)90028-E.

Bloemen, G.W., 1983. Calculation of hydraulic conductivities and steady state capillary rise in peat soils from bulk density and solid matter volume. Zeitschrift für Pflanzenernährung und Bodenkd. 146, 460–473. https://doi.org/10.1002/jpln.19831460407.

Brown, C.M., Strack, M., Price, J.S., 2017. The effects of water management on the CO 2 uptake of Sphagnum moss in a reclaimed peatland. Mires Peat 20, 1–15. https://doi.org/10.19189/MaP.2016.OMB.258.

Crochemore, L., Perrin, C., Andréassian, V., Ehret, U., Seibert, P., Grimaldi, S., Gupta, H., Paturel, J., 2015. Comparing expert judgement and numerical criteria for hydrograph evaluation. Hydrol. Sci. J. 60, 402–423. https://doi.org/10.1080/02626667.2014.903331.

da Silva, F.F., Wallach, R., Chen, Y., 1993. Hydraulic properties of sphagnum peat moss and tuff (scoria) and their potential effects on water availability. Plant Soil 154, 119–126. https://doi.org/10.1007/BF00011080.

Daniel, C., Woods, F.S., 1980. Fitting Equations to Data: Computer Analysis of Multifactor Data. John Wiley Sons Inc.

Dettmann, U., Bechtold, M., Frahm, E., Tiemeyer, B., 2014. On the applicability of unimodal and bimodal van Genuchten-Mualem based models to peat and other organic soils under evaporation conditions. J. Hydrol. 515, 103–115. https://doi.org/10.1016/j.jhydrol.2014.04.047.

Dixon, S.J., Kettridge, N., Moore, P.A., Devito, K.J., Tilak, A.S., Petrone, R.M., Mendoza, C.A., Waddington, J.M., 2017. Peat depth as a control on moss water availability under evaporative stress. Hydrol. Process. 31, 4107–4121. https://doi.org/10.1002/hyp.11307.

Flanagan, T.G.W.-L.B., 1996. Effect of changes in water content on photosynthesis, transpiration and discrimination against 13C02 and C180160 in Pleurozium and Sphagnum. Oecologia 2, 38–46.

Gaudig, G., Krebs, M., Prager, A., Wichmann, S., Barney, M., Caporn, S.J.M., Emmel, M., Fritz, C., Graf, M., Grobe, A., Pacheco, S.G., 2018. Sphagnum farming from species selection to the production of growing media : a review 20, 1–30. https://doi.org/10.19189/MaP.2018.OMB.340.

Gauthier, T.L.J., McCarter, C.P.R., Price, J.S., 2018. The effect of compression on Sphagnum hydrophysical properties: Implications for increasing hydrological connectivity in restored cutover peatlands. Ecohydrology 11, 1–11. https://doi.org/10.1002/eco.2020.

Ghanbarian, B., Hunt, A.G., Ewing, R.P., Sahimi, M., 2013. Tortuosity in Porous Media: A Critical Review. Soil Sci. Soc. Am. J. 77, 1461. https://doi.org/10.2136/sssaj2012.0435.

Gharedaghloo, B., Price, J.S., 2019. Characterizing the immiscible transport properties of diesel and water in peat soil. J. Contam. Hydrol. 221, 11–25. https://doi.org/10.1016/j.jconhyd.2018.12.005.

Gharedaghloo, B., Price, J.S., Rezanezhad, F., Quinton, W.L., 2018. Evaluating the hydraulic and transport properties of peat soil using pore network modeling and X-ray micro computed tomography. J. Hydrol. 561, 494–508. https://doi.org/10.1016/j.jhydrol.2018.04.007.

Gnatowski, T., Szatylowicz, J., Brandyk, T., 2002. Effect of peat decomposition on the capillary rise in peat-moorsh soils from the Biebrza River Valley. Int. Agrophysics 16, 97–102.

Gnatowski, T., Szatyłowicz, J., Brandyk, T., Kechavarzi, C., 2010. Hydraulic properties of fen peat soils in Poland. Geoderma 154, 188–195. https://doi.org/10.1016/j.geoderma.2009.02.021.

Goetz, J.D., Price, J.S., 2015. Role of morphological structure and layering of *Sphagnum* and *Tomenthypnum* mosses on moss productivity and evaporation rates. Can. J. Soil Sci. 95, 109–124. https://doi.org/10.4141/cjss-2014-092.

Golubev, V., 2018. The Effects of Volume Change and Depth/Species Type on the Hydrophysical Properties of Sphagnum Moss. Brandon University.

Golubev, V., Whittington, P.N., 2018. Effects of volume change on the unsaturated hydraulic conductivity of Sphagnum moss. J. Hydrol. 559, 884–894. https://doi.org/10.1016/j.jhydrol.2018.02.083.

Gupta, H.V., Clark, M.P., Vrugt, J.A., Abramowitz, G., Ye, M., 2012. Towards a comprehensive assessment of model structural adequacy. Water Resour. Res. 48, 1–16. https://doi.org/10.1029/2011WR011044.

Hayward, P., Clymo, R.S., 1982. Profiles of water content and pore size in sphagnum and peat, and their relation to peat bog ecology. Proc. R. Soc. London. Ser. B Biol. Sci. 215, 299–325.

Humphreys, E.R., Lafleur, P.M., Flanagan, L.B., Hedstrom, N., Syed, K.H., Glenn, A.J., Granger, R., 2006. Summer carbon dioxide and water vapor fluxes across a range of northern peatlands. J. Geophys. Res. 111. https://doi.org/10.1029/2005JG000111.

Jerauld, G.R., Salter, S.J., 1990. The effect of pore-structure on hysteresis in relative permeability and capillary pressure: pore-level modeling. Transp. Porous Media 5, 103–151.

Kettridge, N., Tilak, A.S., Devito, K.J., Petrone, R.M., Mendoza, C.A., Waddington, J.M., 2016. Moss and peat hydraulic properties are optimized to maximize peatland water use efficiency. Ecohydrology 9, 1039–1051. https://doi.org/10.1002/eco.1708.

Kling, H., Fuchs, M., Paulin, M., 2012. Runoff conditions in the upper Danube basin under an ensemble of climate change scenarios. J. Hydrol. 424–425, 264–277. https://doi.org/10.1016/j.jhydrol.2012.01.011.

Landry, J., Rochefort, L., 2009. Experimental Sphagnum farming station, Shippagan, New Brunswick: Activity report 2003–2008.

Lewis, A.M., 1988. A test of the air-seeding hypothesis using sphagnum hyalocysts. Plant Physiol. 87, 577–582. https://doi.org/10.1104/pp.87.3.577.

Lier, Q.D.J. Van, 2019. Hydrostatic Equilibrium between Soil Samples and Pressure Plates Used in Soil Water Retention Determination: Consequences of a Questionable Assumption 1–14.

Londra, P.A., 2010. Simultaneous determination of water retention curve and unsaturated hydraulic conductivity of substrates using a steady-state laboratory method. HortScience 45, 1106–1112.

Man, H.N., Jing, X.D., 1999. Network modelling of wettability and pore geometry effects on electrical resistivity and capillary pressure 255–267.

McCarter, C.P.R., Ketcheson, S.J., Weber, T.K.D., Whittington, P.N., Scarlett, S., Price, J.S., 2017. Modified Technique for Measuring Unsaturated Hydraulic Conductivity in Sphagnum Moss and Peat. Soil Sci. Soc. Am. J. 81, 747–757. https://doi.org/10.2136/sssaj2007.0111N.

McCarter, C.P.R., Price, J.S., 2015. The hydrology of the Bois-des-Bel peatland restoration: Hydrophysical properties limiting connectivity between regenerated Sphagnum and remnant vacuum harvested peat deposit. Ecohydrology 8, 173–187. https://doi.org/10.1002/eco.1498.

McCarter, C.P.R., Price, J.S., 2014. Ecohydrology of Sphagnum moss hummocks: Mechanisms of capitula water supply and simulated effects of evaporation. Ecohydrology 7, 33–44. https://doi.org/10.1002/eco.1313.

Moore, P.A., Morris, P.J., Waddington, J.M., 2015. Multi-decadal water table manipulation alters peatland hydraulic structure and moisture retention. Hydrol. Process. 29, 2970–2982. https://doi.org/10.1002/hyp.10416.

Moore, P.A., Waddington, J.M., 2015. Modelling Sphagnum moisture stress in response to projected 21st century climate change. Hydrol. Process. 29, 3966–3982. https://doi.org/10.1002/hyp.10484.

Moriasi, D.N., Gitau, M.W., Pai, N., Daggupati, P., 2015. Hydrological and water quality models: performance measures and evaluation criteria. Am. Soc. Agric. Biol. Eng. 58, 1763–1785. https://doi.org/10.13031/trans.58.10715.

Morvannou, A., Forquet, N., Vanclooster, M., Molle, P., 2013. Characterizing hydraulic properties of filter material of a vertical flow constructed wetland. Ecol. Eng. 60, 325–335. https://doi.org/10.1016/j.ecoleng.2013.06.042.

Mualem, Y., 1976. A new model for predicting the hydraulic conductivity of unsaturated porous media. Water Resour. Res. 12, 564–566. https://doi.org/10.1029/WR012i003p00564.

Naasz, R., Michel, J.-C., Charpentier, S., 2005. Measuring hysteretic hydraulic properties of peat and pine bark using a transient method. Soil Sci. Soc. Am. J. 69, 13. https://doi.org/10.2136/sssaj2005.0013.

Nash, J.E., Sutcliffe, J.V., 1970. River flow forecasting through conceptual models Part I-a discussion of principles*. J. Hydrol. 10, 282–290. https://doi.org/10.1016/0022-1694(70)90255-6.

Peters, A., Durner, W., Wessolek, G., 2011. Consistent parameter constraints for soil hydraulic functions. Adv. Water Resour. 34, 1352–1365. https://doi.org/10.1016/j.advwatres.2011.07.006.

Petrone, R.M., Devito, K.J., Silins, U., Mendoza, C., Brown, S.C., Kaufman, S.C., Price, J.S., 2008. Transient peat properties in two pond-peatland complexes in the sub-humid Western Boreal Plain, Canada. Mires Peat 3, 1–13.

Petrone, R.M., Price, J.S., Waddington, J.M., Von Waldow, H., 2004. Surface moisture and energy exchange from a restored peatland, Canada. J. Hydrol. 295, 198–210. https://doi.org/10.1016/j.jhydrol.2004.03.009.

Pouliot, R., Hugron, S., Rochefort, L., 2015. Sphagnum farming: A long-term study on producing peat moss biomass sustainably. Ecol. Eng. 74, 135–147. https://doi.org/10.1016/j.ecoleng.2014.10.007.

Price, J.S., 1992. Blanket bog in Newfoundland. Part 2. Hydrological processes. J. Hydrol. 135, 103–119. https://doi.org/10.1016/0022-1694(92)90083-8.

Price, J.S., Rochefort, L., Quinty, F., 1998. Energy and moisture considerations on cutover peatlands: Surface microtopography, mulch cover and Sphagnum regeneration. Ecol. Eng. 10, 293–312. https://doi.org/10.1016/S0925-8574(98)00046-9.

Price, J.S., Whittington, P.N., 2010. Water flow in Sphagnum hummocks: Mesocosm measurements and modelling. J. Hydrol. 381, 333–340. https://doi.org/10.1016/j.jhydrol.2009.12.006.

Price, J.S., Whittington, P.N., Elrick, D.E., Strack, M., Brunet, N., Faux, E., 2008. A Method to Determine Unsaturated Hydraulic Conductivity in Living and Undecomposed Moss. Soil Sci. Soc. Am. J. 72, 487. https://doi.org/10.2136/sssaj2007.0111N.

Priestley, C.H., Taylor, R.J., 1972. On the assessment of surface heat flux and evaporation using large-scale parameters. Mon. Weather Rev. 100, 81–92. https://doi.org/10.1175/1520-0493(1972) 100<0081:OTAOSH>2.3.CO;2.

R Core Team, 2018. R: A Language and Environment for Statistical Computing.

Reeve, A.S., Siegel, D.I., Glaser, P.H., 2000. Simulating vertical flow in large peatlands. J. Hydrol. 227, 207–217. https://doi.org/10.1016/S0022-1694(99)00183-3.

Schaap, M.G., Leij, F.J., 2000. Improved prediction of unsaturated hydraulic conductivity

with the Mualem-van Genuchten model. Soil Sci. Soc. Am. J. 64, 843–851.
Schelle, H., Heise, L., Jänicke, K., Durner, W., 2013. Water retention characteristics of soils over the whole moisture range: A comparison of laboratory methods. Eur. J. Soil Sci. 64, 814–821. https://doi.org/10.1111/ejss.12108.
Schwärzel, K., Šimůnek, J., Stoffregen, H., Wessolek, G., van Genuchten, M.T., 2006a. Estimation of the unsaturated hydraulic conductivity of peat Soils. Vadose Zo. J. 5, 628. https://doi.org/10.2136/vzj2005.0061.
Schwärzel, K., Šimůnek, J., Van Genuchten, M.T., Wessolek, G., 2006b. Measurement and modeling of soil-water dynamics and evapotranspiration of drained peatland soils. J. Plant Nutr. Soil Sci. 169, 762–774. https://doi.org/10.1002/jpln.200621992.
Sherwood, J.H., Kettridge, N., Thompson, D.K., Morris, P.J., Silins, U., Waddington, J.M., 2013. Effect of drainage and wildfire on peat hydrophysical properties. Hydrol. Process. 27, 1866–1874. https://doi.org/10.1002/hyp.9820.
Silvola, J., 1990. Combined effects of varying water content and CO2 concentration on photosynthesis in Spagnum fuscum. Holartic Ecol. 13, 224–228.
Simhayov, R.B., Weber, T.K.D., Price, J.S., 2018. Saturated and unsaturated salt transport in peat from a constructed fen. Soil 4, 63–81.
Šimůnek, J., Hopmans, J.W., 2002. Parameter Optimization and Nonlinear Fitting. In: Dane, J.H., Topp, C.G., (Eds.), Methods of Soil Analysis: Part 4 Physical Methods. SSSA, Madison, WI, pp. 139–157. https://doi.org/10.2136/sssabookser5.4.c7.
Šimůnek, J., Sejna, M., Saito, H., Sakai, M., van Genuchten, M.T., 2009. "The HYDRUS-1D software package for simulating the one-dimensional movement of water, heat, and multiple solutes in variably-saturated media. Version 4.08. HYDRUS Softw. Ser. 3. Dep. Environ. Sci., Univ. Calif., Riverside.
Šimůnek, J., van Genuchten, M.T., Šejna, M., 2012. HYDRUS: Model Use, Calibration, and Validation. Trans. ASABE 55, 1263–1276. https://doi.org/10.13031/2013.42239.
Strack, M., Price, J.S., 2010. Moisture controls on carbon dioxide dynamics of peat-Sphagnum monoliths. Ecohydrology 130, 126–130. https://doi.org/10.1002/eco.
Taylor, N., Price, J.S., 2015. Soil water dynamics and hydrophysical properties of regenerating Sphagnum layers in a cutover peatland. Hydrol. Process. 29, 3878–3892. https://doi.org/10.1002/hyp.10561.
Thompson, D., Waddington, J., 2008. Sphagnum under pressure: towards an ecohydrological approach to examining Sphagnum productivity. Ecohydrology 308, 299–308.
van Genuchten, M.T., 1980. A closed-form equation for predicting the hydraulic conductivity of unsaturated soils1. Soil Sci. Soc. Am. J. https://doi.org/10.2136/sssaj1980.03615995004400050002x.
van Genuchten, M.T., Leij, F.J., Yates, S.R., 1991. In: The RETC Code for Quantifying the Hydraulic Functions of Unsaturated Soils. United States Environ. Research Lab. https://doi.org/10.1002/9781118616871.
Vrugt, J.A., Stauffer, P.H., Wöhling, T., Robinson, B.A., Vesselinov, V.V., 2008. Inverse modeling of subsurface flow and transport properties: a review with new developments. Vadose Zo. J. 7, 843. https://doi.org/10.2136/vzj2007.0078.
Weber, T.K.D., Iden, S.C., Durner, W., 2017a. Unsaturated hydraulic properties of Sphagnum moss and peat reveal trimodal pore-size distributions. Water Resour. Res. 415–434. https://doi.org/10.1002/2016WR019707.Received.
Weber, T.K.D., Iden, S.C., Durner, W., 2017b. A pore-size classification for peat bogs derived from unsaturated hydraulic properties. Hydrol. Earth Syst. Sci. 21, 6185–6200. https://doi.org/10.5194/hess-21-6185-2017.
Weiss, R., Alm, J., Laiho, R., Laine, J., 1998. Modeling moisture retention in peat soils. Soil Sci. Soc. Am. J. 62, 305. https://doi.org/10.2136/sssaj1998.03615995006200020002x.
Zambrano-Bigiarini, M., 2017. hydroGOF: Goodness-of-fit functions for comparison of simulated and observed hydrological time series. https://doi.org/10.5281/zenodo.840087.